Novel Nano-Scale Computing Unit for the IoBNT: Concept and Practical Considerations

Stefan Angerbauer[1], Franz Enzenhofer[2], Tobias Pankratz[2], Medina Hamidovic[2], Andreas Springer[2], and Werner Haselmayr[2]

[1]Johannes Kepler University Linz, Institute for Communications Engineering and RF-Systems, JKU LIT SAL eSPML Lab, Linz, Austria

[2]Institute for Communications Engineering and RF-Systems, Johannes Kepler University Linz, Austria

***Abstract*—The Internet of Bio-Nano Things (IoBNT) is a novel framework that has the potential to enable transformative applications in healthcare and nano-medicine. It consists of artificial or natural tiny devices, so-called Bio-Nano Things (BNTs), that can be placed in the human body to carry out specific tasks (e.g., sensing) and are connected to the internet. However, due to their small size their computation capabilities are limited, which restricts their ability to process data and make decision directly in the human body. Thus, we address this issue and propose a novel nano-scale computing architecture that performs matrix multiplications, which is one of the most important operations in signal processing and machine learning. The computation principle is based on diffusion-based propagation between connected compartments and chemical reactions within some compartments. The weights of the matrix can be set independently through adjusting the volume of the compartments. We present a stochastic and a dynamical model of the proposed structure. The stochastic model provides an analytical solution for the input-output relation in the steady state, assuming slow reaction rates. The dynamical model provides important insights into the systems temporal dynamics. Finally, micro- and mesoscopic simulations verify the proposed approach.**

***Index Terms*—Internet of Bio-Nano Things, Machine Learning, Molecular Communications, Unconventional Computing**

I. Introduction

Delayed diagnosis and treatment of diseases can lead to serious consequences for patients and a significant financial burden on healthcare institutions and companies [2]. For example, the study in [2] lists waiting for test, misdiagnosis and limited access to healthcare as some of the major causes of diagnosis delay. Thus, improvements on these factors will largely influence both the individual and general health state and life expectancy of those parts of the population needing medical attention. Various studies have shown that information and communication technologies (ICT) can have a large positive impact on medical diagnostics and healthcare monitoring [3], [4]. The Internet of Bio-Nano Things (IoBNT) provides such a ICT framework, which aims to connect Bio-Nano Things (BNTs) to the internet [5], [6]. Hence, it paves the way for a more personalized online supervision of a person's health status and faster intervention in the case of illness. Typically, BNTs are tiny machines that can be realized using either nano-technology or synthetic biology (e.g., engineered bacteria) [7]. They can be placed in the human body and are capable of carrying out simple specific tasks, such as sensing the environment, localizing malicious cells or releasing specific molecules (e.g., drugs). However, due to their small size the computation capabilities of BNTs are limited. Nevertheless, there are recent efforts to design nano-scale systems, that are able to execute complex machine learning (ML) algorithms. The increased computation power of BNTs significantly reduces the amount of data that may need to be exchanged with the cyber-domain, since some computations and decisions can be already made inside the human body. This will make the decision making process in IoBNT applications faster and more reliable, as molecular communication (MC) [8], the most promising communication scheme for IoBNT, suffers from low data rates and stochasticity.

One promising approach to realize ML algorithms in the nano-scale is based on genetic engineering of living cells [9], [10]. In [9], genetic engineering is utilized to modify a *E. coli* bacterium in a way that it imitates a neuro-synapse, which is called a bactoneuron. The bactoneuron forms a linear combination of multiple-input chemical concentrations and distorts this result nonlinearly. The output of the computation is obtained by measuring the concentration of a fluorescent protein, which is produced in response to the nonlinearly distorted signal. The bactoneuron can be interpreted as a single layer neural network (NN), which was verified experimentally using various computing tasks. However, the implementation of this approach is quite complex, since it requires genetic engineering and living cells. To overcome the issue of engineering a synthetic circuit from scratch, the method presented in [10] exploits the fact that living cells naturally have gene-regulation networks, which regulate different processes within the cell. The idea is to identify sub-networks within these existing gene-regulation networks, that have the same architecture as the NN to be realized. The weights of this network are set by adjusting the gene expression rates through altering environmental parameters, such as the ambient temperature. While this method requires lower effort in terms of biotechnology, it is highly complex to generate arbitrary NNs, since the individual network weights cannot be chosen independently of each other. Another chemical computation

This manuscript was presented in part at the 2023 IEEE Global Communication Conference [1]

approach for the realization of ML algorithms is proposed in [11], which does not rely on living cells. Microfluidic channels and chemical reactions are utilized to realize logic gates (e.g., AND gate), which form the basis of conventional computers. Compared to [9], [10], the implementation of this approach is easier, but for the realization of NNs a very large number of logic gates is required. This may limit the ability to downscale it to the nano-domain. Finally, there is the concept of chemical reaction networks (CRNs), which conceptually lies between the aforementioned approaches [12], [13]: A cascade of chemical reactions is engineered to perform an intended operation (i.e., neural network inference) within a given volume. The advantage of this approach is, that compared to [9] it provides a higher degree of control over the involved processes, while directly carrying out a matrix multiplication as opposed to [11]. However, due to the large number of required reactions, the concept might become complex for larger structures. In summary, the main limitations for the implementation of ML algorithms at nano-scale are the implementation complexity (cf. [9], [10]) and the lack in downscaling to the nano-domain (cf. [11]).

In this work, we present a novel nano-scale computing architecture that is capable of performing matrix multiplications, which is the basic operation for the realization of a single layer NN[2]. The proposed architecture overcomes the limitations of the aforementioned approaches, since it does not require living cells and enables an efficient implementation at the nano-domain. The structure consists of connected compartments and the computation principle is based on diffusion-based propagation between these compartments and chemical reactions within some compartments. The weights of the matrix can be set independently by adjusting the volume of the compartments. It is important to note that the proposed computing architecture requires no external stimulus. The main contributions of this work can be summarized as follows (cf. Fig. 1):

1) We present a novel nano-scale computing architecture that performs matrix multiplications, which builds the basis for many signal processing and ML algorithms.
2) We provide a stochastic model, which gives an analytical solution for the input-output relation in the steady state, assuming slow reaction rates. This model allows to define a noise model and a naive design algorithm for the compartment volumes given arbitrary matrix weights.
3) We provide a dynamical model, which fully characterizes the dynamic behavior of the proposed structure using systems of coupled ordinary differential equations. Compared to the stochastic model it has no constraints (e.g., slow reaction) and enables the derivation of important system insights, such as the computation speed. This model leads to an advanced design algorithm for the compartment volumes.
4) We verify the functionality of the presented structure and the corresponding models using a microscopic-mesoscopic hybrid simulation.

[2]The realization of multi-layer NNs is out of scope of this work and will be investigated in a future work.

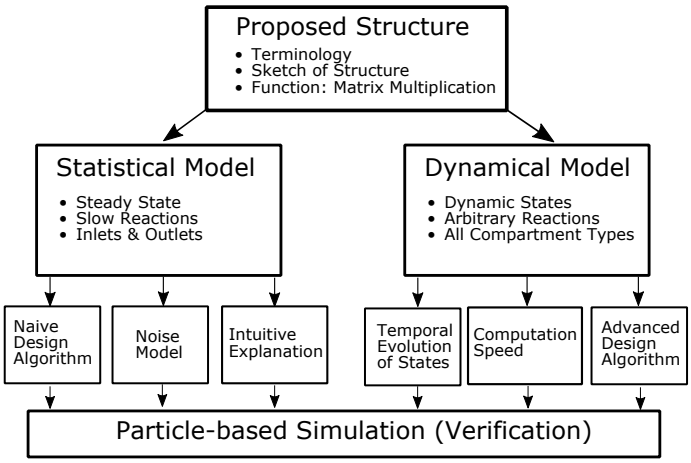

Fig. 1. Overview of the main contributions

The remainder of this work is organized as follows: Sec. II introduces the proposed structure and the used terminology and notation. A stochastic model is presented in Sec. III, which gives first insights into the working principle of the structure. Moreover, a naive design algorithm for the compartment volumes is presented. Sec. IV presents a dynamical model and provides an estimate of the computation speed. In Sec. V an advanced design algorithm for the compartments volumes is derived. We verify our models and the proposed models using a microscopic-mesoscopic hybrid simulation in Sec. VI and provide a conclusion and outlook in Sec. VII.

II. Terminology and Notation of the Proposed Architecture

In this section, we introduce the proposed structure and notation for its description.

A. Description of the Structure

To introduce the nomenclature used for different parts of the structure, we consider the sketch of a realization for a 2×2-matrix multiplication in Fig. 2. The circles indicate compartments, which are reservoirs with well defined volume and content. The top row of compartments are called inlet-compartments (or inlets), the second row compartments are called intermediate compartments (or intermediates) and the bottom row are called outlet compartments (or outlets). The connecting lines indicate channels, which link compartments to one another. Through these channels molecules can spread via diffusion. We index inlets with $i \in I$, intermediates with (i, j) and outlets with $j \in J$. The variables written in sanserif indicate the molecule types, e.g., A corresponds to molecules of type A. The arrows to the left and right of the structure indicate the type of molecule, that is able to spread in this direction. The molecule type in a compartment is indicated by the same variable, i.e., in the inlets only A molecules can be found, in the intermediates A-type molecules are converted to B-type molecules and in the outlets only B-type molecules can be found. It is important to note that $\mathsf{B} \in \{\mathsf{B}^+, \mathsf{B}^-\}$, i.e., A can be converted into two different types of B molecules, where B^+ is used to realize positive and B^- to realize negative

numbers (see Sec. II-C). Furthermore, we distinguish signaling molecules and auxiliary molecules. Signaling molecules are A and B-type molecules, i.e., molecules, that are able to propagate across the structure and change over time. On the other hand auxiliary molecules are molecules, that are neither input nor output of the reaction, but might affect parameters of the process, such as the reaction rate. They are assumed to have a (almost) constant concentration over time. In this work we only consider two types of auxiliary molecules, namely C^+ and C^-. Their properties are

- Constant over time
- Only present in the intermediates and unable to diffuse anywhere else
- Exactly one of them is found in each intermediate, depending on the intended sign of the respective weight (see Sec. II-C)

B. Notation for States

Throughout this work, we will use state-space models to keep track of the movement of all molecules within the structure. These models can either be formulated in terms of concentrations or number of molecules, with each of the two being a valid representation of the state of a compartment. In this subsection we introduce the respective notation. We use V to indicate the volumes of compartments. By convention, inlet compartments have the index "in, i" (i.e., $V_{\mathrm{in},i}$ is the volume of the i-th inlet compartment), intermediates the index "i, j" (i.e., the intermediate connecting i-th inlet to j-th outlet has volume $V_{i,j}$) and outlets the index "out, j" (i.e., $V_{\mathrm{out},j}$ is the volume of the j-th outlet compartment). This notation also holds for the number of molecules N and concentration of molecules C, which are linked by

$$N = CV. \tag{1}$$

However, for N and C, in addition to indicate the compartment, we also have to specify the molecule type, which is done using a superscript. For example, $N^{\mathsf{A}}_{\mathrm{in},1} = C^{\mathsf{A}}_{\mathrm{in},1} V_{\mathrm{in},1}$ describes the relationship between the number and concentration of A-type molecules in the first inlet compartment. Note, that all numbers of molecules and concentrations are in general functions of time. We will however omit the time dependence for the sake of readability. The initial and final concentration in a compartment, on the other hand does not depend on time. It is marked by additional superscripts "init" or "fin", respectively (i.e., $N^{\mathsf{A},\mathrm{init}}_{\mathrm{in},1}$ is the number of molecules initially placed in the first inlet compartment and $C^{\mathsf{B},\mathrm{fin}}_{\mathrm{out},2}$ is the concentration of B molecules in the second outlet). Finally, we use lower case variables to indicate random variables (i.e., $c^{\mathsf{B},\mathrm{fin}}_{\mathrm{out},2}$). If the random variable is normally distributed, the corresponding upper case variable can be interpreted as its expected value (i.e., $C^{\mathsf{B},\mathrm{fin}}_{\mathrm{out},2}$ is the expected value of $c^{\mathsf{B},\mathrm{fin}}_{\mathrm{out},2}$).

C. Notation for Transport Processes

The propagation of molecules through the structure is driven by two major physical processes, with the first being diffusion (transport between compartments) and the second one reaction (transfer between species). Diffusion describes the passive process of distribution of molecules between compartments due to Brownian motion. The property of the propagation medium is thereby reflected by the diffusion coefficient D. As will be shown later, further parameters influencing this process are the volumes of the compartments, the channel cross section area S and length d. Reactions, on the other hand, refer to the conversion of molecules from one type to another. The reactions taking place in our structure are

$$\mathsf{A} + \mathsf{C}^+ \rightarrow \mathsf{B}^+, \tag{2}$$

$$\mathsf{A} + \mathsf{C}^- \rightarrow \mathsf{B}^-, \tag{3}$$

and

$$\mathsf{B}^+ + \mathsf{B}^- \rightarrow *. \tag{4}$$

Note, that since each intermediate contains exactly one of the two molecule types C^+ and C^-, only one of the two reactions (2) and (3) takes place in these compartments. The reaction (4) takes place, if an outlet receives molecules of both B-molecule types (i.e., if the respective outlet is connected to at least one intermediate of each reaction type (2) and (3)). The $*$ indicates one or multiple species, which we are not interested in and therefore do not count their respective number of molecules. It is important, that this species does not react with any signaling molecule and furthermore does not impact the propagation of signaling molecules.

We assume, that all three above equations happen at the same rate. For the speed of a reaction the parameters r (second order reaction) and k (first order reaction) are used. For both reaction and diffusion, we will define respective fluxes. Since diffusive fluxes leave one compartment and go into another one, we will adopt the index "$\mathrm{source} \rightarrow \mathrm{sink}$" (i.e., $F^{\mathsf{A}}_{\mathrm{in}\rightarrow(i,j)}$ is the flux of A-type molecules going from inlet i to intermediate (i, j)). Since diffusive fluxes always spread either between inlet and intermediate or intermediate and outlet, the index of the inlet/outlet compartment is obvious from (i, j) and is thereforee neglected (e.g., we do not write $F^{\mathsf{A}}_{(\mathrm{in},i)\rightarrow(i,j)}$, but $F^{\mathsf{A}}_{\mathrm{in}\rightarrow(i,j)}$). We use F_{re} to indicate reactive fluxes.

III. Stochastic Model

In this section, we derive the relation between input and output concentration of the proposed structure and show, that it can be formulated as a matrix multiplication. We start by an intuitive physical explanation. Then, we employ a stochastic modeling approach to formulate the intuitive explanation in mathematical terms.

A. Working Principle – Intuitive Explanation

In this section, we provide an intuitive description of the working principle of the proposed structure. We start our discussion by just considering the first inlet and the connected intermediates $(1, 1)$ and $(1, 2)$ as shown in Fig. 2 and extend this to more inlets later. At the beginning of the computation, a certain number of A-type molecules $N^{\mathsf{A}}_{\mathrm{in},1}$ is placed in the inlet, which corresponds to the concentration $C^{\mathsf{A}}_{\mathrm{in},1} = N^{\mathsf{A}}_{\mathrm{in},1}/V_{\mathrm{in},1}$.

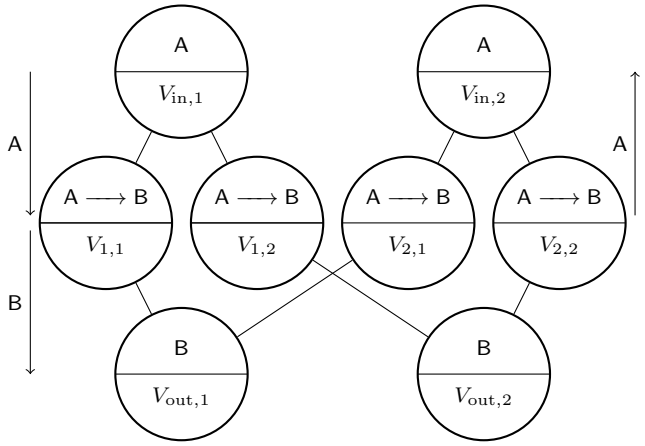

Fig. 2. System architecture of a 2×2 matrix multiplication. Inlet, intermediate, and outlet compartments are shown at the top, middle, and bottom.

Assuming that the influence of the reactions in the intermediates can be neglected for now, this initial number of molecules will diffuse to the intermediates, until all three compartments have the same concentration, i.e., $N^{\mathsf{A}}_{\mathrm{in},1}/(V_{\mathrm{in},1}+V_{1,1}+V_{1,2})$. After the three compartments have reached the equilibrium, we now consider the reaction in the intermediates. If this reaction is slow compared to the diffusion, we can assume that also in the presence of the reaction, the inlet and its connected intermediates have the same concentration. However, due to the conversion of A-type molecules in the intermediates the overall number of molecules in the joint volume of inlet and intermediate compartments will decay over time. This process continues until all A-type molecules initially placed in the inlet have been converted by reaction in the intermediates.

Next, we discuss the probability that an A-type molecule is converted in one specific intermediate using the following example: If the volume of the intermediate $(1,1)$ is twice as large as the volume of the intermediate $(1,2)$, i.e., $V_{1,1}=2V_{1,2}$, the probability that a molecule is in $(1,1)$ is twice than in $(1,2)$. The reason for that is that although the concentrations are the same, larger volumes have a larger number of expected molecules. Thus, the probability of a molecule being converted in $(1,1)$ is twice the probability of being converted in $(1,2)$, which results in the probabilities $2/3$ and $1/3$, respectively. Once a molecule has been converted, it ends up in the corresponding outlet with probability one, e.g., all molecules converted in $(1,2)$ end up in outlet 2 (cf. Fig. 1). It is important to note that the aforementioned fraction of molecules can be interpreted as the fraction of molecules placed in the first inlet ending up in either outlet 1 or 2, e.g., the fraction of molecules ending up in outlet 2 is given by $1/3$. In other words, the number of molecules in a certain outlet corresponds to the number of molecules in the inlet times a certain weight (fraction) that is determined by the intermediate volumes. However, since the fractions are always less than or equal to one, we need some additional design parameters to realize arbitrary weights. So far, we have only considered intermediate volumes for the design. In order to realize arbitrary weights the appropriate choice of the inlet and outlet volumes is also crucial. Let's assume that we would like to realize the weights 2 and 1. In this case the inlet volume must be chosen three times the outlet volume, which will be justified below. According to the discussion above, from $N_{\mathrm{in},1}=C_{\mathrm{in},1}V_{\mathrm{in},1}$ molecules initially placed in the first inlet, $2/3$ will end up in intermediate $(1,1)$ and further in outlet 1, which results in the outlet concentration $2/3C_{\mathrm{in},1}V_{\mathrm{in},1}/V_{\mathrm{out},1}$. Since $V_{\mathrm{in},1}/V_{\mathrm{out},1}=3$, we obtain the desired weight of 2. Similar considerations can be made for outlet 2, resulting in the weight 1. From this example we can infer the following connection between intended weights and volumes of the structure:

- The ratio of the weights defines the ratio of the intermediate volumes (or vice versa)
- Since the ratio of the weights to one another was set in the previous step, they can differ from the intended value at most by a multiplicative factor which can be adjusted by setting the ratio of inlet to outlet volume appropriately.

A more detailed mathematical description of these observations will be presented in (20). As mentioned at the beginning of the section, the description above only considers the effect of one inlet on the corresponding outlets. However, the total concentration in the outlets can be obtained through the superposition of the effects of all inlets.

Finally, we provide an explanation on how to realize negative weights. Therefore, we use the molecules C^+ and C^- and B^+ and B^-, respectively. If an intermediate is filled with C^+ molecules it generates B^+ molecules (cf. (2)) and the same holds for C^- and B^- molecules (cf. (3)). Thus, the sign of the molecules coming from one intermediate compartment can be controlled by choosing the respective C. Since the B molecules react in the outlets according to (4), which stops only if one of the two species is used up entirely, only the surplus of either of the two species remains. Thus, if at the end only B^+ molecules remain, their concentration encodes a positive number, otherwise the remaining concentration of the B^- molecules encodes a negative number.

B. Mathematical Explanation

In this subsection, based on the discussion before, we will describe the working principle of the structure mathematically. The overall goal is to multiply an input vector $\boldsymbol{C}_{\mathrm{in}}$ (which is encoded in the A-type molecules concentrations of the inlets) by a matrix $\boldsymbol{M}$ to obtain an output vector $\boldsymbol{C}_{\mathrm{out}}$ (encoded in the B-type concentration in the outlet compartments), i.e.,

$$\boldsymbol{C}_{\mathrm{out}}=\boldsymbol{M}\boldsymbol{C}_{\mathrm{in}}. \tag{5}$$

This is achieved by choosing the content and volumes of the structure appropriately. Please note that for the sake of readability, we will use the term "B-molecules" instead of "B^--" and "B^+-molecules", in the following. The same convention is used for the C-type molecules. Where necessary, we will introduce the sign $s_{i,j}$ to enable a distinction.
For the following derivations, we make two assumptions:

- The reaction rate is small (compared to the rate of diffusion), but not zero. Moreover, please note that when we state diffusion is fast or reaction is slow, it is always with respect to the other process.
- We neglect the first time interval, in which diffusion equilibrates the concentration of an inlet and its connected

intermediates. It will be short compared to the time the reaction takes since we assumed that diffusion is much faster than reaction

The initial signal molecule concentrations of all non-inlet compartment is assumed to be zero at the beginning of a computation. Note that C molecules are not considered as signaling molecules and their concentration is set to a fixed concentration $C_{i,j}^{\mathsf{C}^+,\text{init}}$ and $C_{i,j}^{\mathsf{C}^-,\text{init}}$ depending on the sign. All intermediates with the same sign have the same concentration of C-type molecules.

We assume that the initial concentrations in the inlets are set instantaneously at the beginning of a computation. Based on the above assumption, the concentration between one inlet and its J intermediates is equalized after a short time (which we neglect). This can be mathematically written as $C_{\text{in},k}^{\mathsf{A}} = C_{i,j}^{\mathsf{A}}|_{i=k} \forall j \in J$. If we assume a first order forward reaction in the intermediate compartments (which is valid if the concentration of C^+ and C^- in (3) and (4) is sufficiently large, as will be shown later) the concentration of A-molecules $C_{i,j}^{\mathsf{A}}(t)$ and number of B-molecules $N_{i,j}^{\mathsf{B}}(t)$ generated therein are related by

$$\frac{dN_{i,j}^{\mathsf{B}}}{dt} = V_{i,j} k C_{i,j}^{\mathsf{A}}, \tag{6}$$

Integrating this equation with respect to time gives the overall number of B molecules generated in intermediate (i,j). Since, due to the unidirectional transport from intermediate to outlet, each of these molecules will end up in outlet j, we can formulate the number of molecules in the j-th outlet only due to the effect of the $i=k$-th inlet ($k \in [1, I]$) as

$$N_{\text{out},j}^{\mathsf{B},\text{fin}}|_{i=k} = \int_0^\infty V_{i,j} k C_{i,j}^{\mathsf{A}} dt \tag{7}$$

Considering that all molecules initially placed in an inlet $i=k$ will be converted in one intermediate as time approaches infinity, we obtain

$$N_{\text{in},k}^{\mathsf{A},\text{init}} = \int_{t=0}^\infty \sum_{j=1}^{J} F_{\text{in}\to(k,j)}^{\mathsf{A}} dt \tag{8}$$

Combining (7) and (8) we get the fraction of molecules from $i=k$-th inlet ending up in j-th outlet as

$$\begin{aligned}\frac{N_{\text{out},j}^{\mathsf{B},\text{fin}}|_{i=k}}{N_{\text{in},k}^{\mathsf{A},\text{init}}} &= \frac{\int_{t=0}^\infty F_{(k,j)\to\text{out}}^{\mathsf{B}} dt}{\int_{t=0}^\infty \sum_{j=1}^{J} F_{\text{in}\to(k,j)}^{\mathsf{A}} dt} \\ &= \frac{V_{k,j}\int_{t=0}^\infty k C_{k,j}^{\mathsf{A}} dt}{\sum_{j=1}^{J} V_{k,j}\int_{t=0}^\infty k C_{k,j}^{\mathsf{A}} dt}.\end{aligned} \tag{9}$$

As mentioned above, the concentrations of all intermediates connected to the same inlet have the same concentration. Therefore, the integrals in (9) yield the same result and it simplifies to

$$\chi_{k,j} = \frac{N_{\text{out},j}^{\mathsf{B},\text{fin}}|_{i=k}}{N_{\text{in},k}^{\mathsf{A},\text{init}}} = \frac{V_{k,j}}{\sum_{j=1}^{J} V_{k,j}}. \tag{10}$$

We can interpret $\chi_{k,j}$ as the probability of a molecule initially placed in inlet k ending up in outlet j. Consequently, if initially $N_{\text{in},i}^{\mathsf{A},\text{init}} = V_{\text{in},i} C_{\text{in},i}^{\mathsf{A},\text{init}}$ were placed in the k-th inlet, the final number of molecules in the j-th outlet will be distributed according to

$$n_{\text{out},j}^{\mathsf{B},\text{fin}}\big|_{i=k} \sim \mathcal{B}\left(V_{\text{in},k} C_{\text{in},k}^{\mathsf{A},\text{init}}, \chi_{k,j}\right), \tag{11}$$

where $\mathcal{B}(n,p)$ denotes the Binomial distribution with n the number of independent trials and p the probability of success. Note that we used a lower case variable to indicate a random variable. Given that the number of molecules is large we can use the De Moivre–Laplace theorem [14] to obtain

$$\begin{aligned}&\mathcal{B}\left(V_{\text{in},k} C^{\mathsf{A}}, \chi_{k,j}\right) \approx \\ &\mathcal{N}\left(V_{\text{in},k} C_{\text{in},k}^{\mathsf{A},\text{init}} \chi_{k,j}, V_{\text{in},k} C_{\text{in},k}^{\mathsf{A},\text{init}} \chi_{k,j}\left(1-\chi_{k,j}\right)\right).\end{aligned} \tag{12}$$

Thereby, $\mathcal{N}\left(\mu, \sigma^2\right)$ indicates the normal distribution with expected value μ and standard deviation σ. Since the inlets are independent of each other, the overall distribution of the number of molecules in the j-th outlet follows as [14]

$$n_{\text{out},j}^{\mathsf{B},\text{fin}} = \sum_{k=1}^{I} n_{\text{out},j}^{\mathsf{B},\text{fin}}\big|_{i=k} \sim \mathcal{N}\left(\overline{\mu}_j, \overline{\sigma}_j^2\right), \tag{13}$$

with $\overline{\mu}_j = \sum_{k=1}^{I} s_{k,j} V_{\text{in},k} C_{\text{in},k}^{\mathsf{A},\text{init}} \chi_{k,j}$, $\overline{\sigma}_j^2 = \sum_{k=1}^{I} V_{\text{in},k} C_{\text{in},k}^{\mathsf{A},\text{init}} \chi_{k,j}(1-\chi_{k,j})$ and $s_{k,j} \in \{-1, 1\}$ indicating the sign of the (k,j)-th intermediate. The distribution of the concentration can be obtained by dividing mean and standard deviation by the outlet volume $V_{\text{out},1} = V_{\text{out},2} = V$ resulting in

$$c_{\text{out,j}}^{\mathsf{B},\text{fin}} \sim \mathcal{N}\left(\mu_j, \sigma_j^2\right), \tag{14}$$

with $\mu_j = \frac{\overline{\mu_j}}{V}$ and $\sigma_j^2 = \frac{\overline{\sigma}_j^2}{V^2}$.

C. Interpretation of the Stochastic Model

Reconsidering the mean of the probability distribution in (14) we can write

$$C_{\text{out},j}^{\mathsf{B},\text{fin}} = \frac{1}{V}\sum_{k=1}^{I} s_{k,j}\chi_{k,j} V_{\text{in},k} C_{\text{in},k}^{\mathsf{A},\text{init}} = \sum_{k=1}^{I} w_{k,j} C_{\text{in},k}^{\mathsf{A},\text{init}}. \tag{15}$$

Collecting all $C_{\text{out},j}^{\mathsf{B},\text{fin}}$ in the vector $\boldsymbol{C}_{\text{out}}$ (dimension $J \times 1$) and all $C_{\text{in},i}^{\mathsf{A},\text{init}}$ in the vector $\boldsymbol{C}_{\text{in}}$ (dimension $I \times 1$), we can rewrite (15) in matrix-vector notation

$$\boldsymbol{C}_{\text{out}} = \boldsymbol{W}\boldsymbol{C}_{\text{in}}, \tag{16}$$

with the matrix $\boldsymbol{W}$ (dimension $J \times I$) having the following entry in the j-th row and k-th column $W_{j,k} = w_{k,j}$; please note here the flip of the index positions. Thus, we have proven that the proposed structure is capable of realizing a matrix multiplication, as we demanded in (5). In the next step, we show that it is possible to set $\boldsymbol{W}$ to any arbitrary desired matrix $\boldsymbol{M}$. Thus, we demand $\boldsymbol{M} = \boldsymbol{W}$ or equivalently

$$M_{j,i} = w_{i,j} = \frac{s_{i,j} V_{i,j} V_{\text{in},i}}{V \sum_{i=1}^{I} V_{i,j}}, \tag{17}$$

with the desired weight $M_{j,i}$ that depends on multiple volumes in the structure. Note that this equation gives $M_{j,i}$ as a function of the volumes. When we want to design a structure, however, we want the opposite, namely the volumes as a function of the

weights to be realized. To obtain this relationship, such that (17) holds for all $M_{j,i}$, we consider a simple example of a 2×2 matrix and demand that

$$\begin{bmatrix} M_{1,1} & M_{1,2} \\ M_{2,1} & M_{2,2} \end{bmatrix} = \begin{bmatrix} \frac{s_{1,1}V_{1,1}V_{\mathrm{in},1}}{(V_{1,1}+V_{1,2})V} & \frac{s_{2,1}V_{2,1}V_{\mathrm{in},2}}{(V_{2,1}+V_{2,2})V} \\ \frac{s_{1,2}V_{1,2}V_{\mathrm{in},1}}{(V_{1,1}+V_{1,2})V} & \frac{s_{2,2}V_{2,2}V_{\mathrm{in},2}}{(V_{2,1}+V_{2,2})V} \end{bmatrix}, \tag{18}$$

with arbitrary real valued numbers $M_{j,i}$. Obviously, this problem is solved by setting $V_{\mathrm{in},1} = |M_{1,1}| + |M_{2,1}|$, $V_{\mathrm{in},2} = |M_{1,2}| + |M_{2,2}|$, $V_{1,1} = |M_{1,1}|$, $V_{1,2} = |M_{2,1}|$, $V_{2,1} = |M_{1,2}|$, $V_{2,2} = |M_{2,2}|$ and $V = 1$, which results in

$$\boldsymbol{M} = \begin{bmatrix} \frac{M_{1,1}(|M_{1,1}|+|M_{2,1}|)}{|M_{1,1}|+|M_{2,1}|} & \frac{M_{1,2}(|M_{1,2}|+|M_{2,2}|)}{|M_{1,2}|+|M_{2,2}|} \\ \frac{M_{2,1}(|M_{1,1}|+|M_{2,1}|)}{|M_{1,1}|+|M_{2,1}|} & \frac{M_{2,2}(|M_{1,2}|+|M_{2,2}|)}{|M_{1,2}|+|M_{2,2}|} \end{bmatrix}. \tag{19}$$

Please note that $M_{j,i}$ is defined as $M_{j,i} = \mathrm{sgn}(M_{j,i})|M_{j,i}|$, and $\mathrm{sgn}(M_{j,i})$ is considered through the choice of $\mathsf{C} \in \{C^+, C^-\}$. From (19) we notice that there are infinitely many solutions realizing the same matrix. If for example all inlet volumes ($V_{\mathrm{in},1}$ and $V_{\mathrm{in},2}$) and outlet volumes V are doubled, we obtain the same result. Thus, we conclude that there are infinitely many solutions to the problem, which are equally good as long as diffusion is much faster than reaction and we do not want to impose other constraints on our solution (i.e., constraints on the largest allowed volume, computation duration etc.).

The line of argumentation presented above for the 2×2 matrix extends to higher matrix dimensions in a straightforward way: Assuming a desired matrix $\boldsymbol{M}$ with dimension $J \times I$, we always find at least one realization (again, there are infinitely many) by choosing the volumes as follows

$$V_{\mathrm{in},i} = \sum\nolimits_{k=1}^{J} |M_{k,i}| \tag{20a}$$
$$V_{i,j} = |M_{j,i}| \tag{20b}$$
$$s_{i,j} = \mathrm{sign}(M_{j,i}) \tag{20c}$$
$$V = 1, \tag{20d}$$

where $s_{i,j}$ corresponds to the content of the (i,j)-intermediate (i.e., C^+ or C^-). We will refer to this way of determining the volumes of the structure as Naive Design Algorithm in the remaining work, since it was calculated using the naive assumption, that diffusion is much faster than reaction. Please note that the volumes are just a function of the weights and no knowledge about the channel shape, the speed of reaction, or the diffusion coefficient is required. The physical reason for this behavior of the system will be shown in Sec. V-A. Finally, let's revisit the standard deviation of the number of outlet molecules given in (13), which is a measure for the uncertainty of the output and reads as

$$\sigma_j = \sqrt{\frac{1}{V^2} \sum_{k=1}^{I} \chi_{k,j}(1-\chi_{k,j}) V_{\mathrm{in},k} C_{\mathrm{in},k}^{\mathsf{A},\mathrm{init}}}. \tag{21}$$

From the definition of the standard deviation we can observe two interesting properties: Firstly, it does not depend on the sign (i.e., auxiliary molecules) of the compartment and secondly, we notice that the standard deviation is also a function of the concentration, i.e., a larger initial input concentration leads to larger standard deviation of the computation. Finally, it should be noted that V affects the variance inversely quadratic. As we have shown previously, the realized matrix is defined by $\chi_{k,j}$ and $\frac{V_{\mathrm{in},k}}{V}$. Hence, for the same matrix, we can change the variance of the computation by choosing $V_{\mathrm{in},k}$ and V in the same ratio, but with larger absolute value to reduce the variance/standard deviation of the computation.

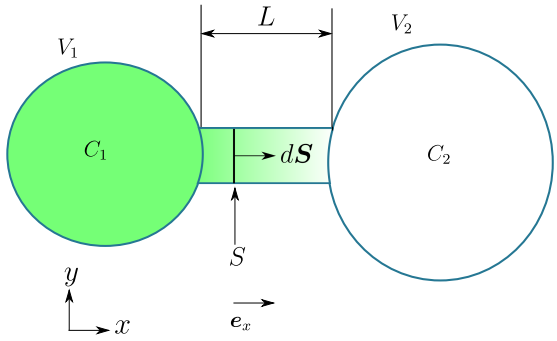

Fig. 3. Diffusion through two interconnected compartments.

IV. Dynamic Model

In the previous section, we utilized the assumption, that diffusion is much faster than the reactions taking place in the intermediate compartments. However, in a practical setup, this condition may be violated and, thus, more detailed models to analyze the effect of this violation are needed. Therefore, in this section, we derive a dynamical model of the proposed structure allowing for a detailed model of the temporal evolution of the system states.

A. Fundamentals

In order to model the structure depicted in Fig. 2, we utilize a set of differential equations, commonly referred to as compartment models. These differential equations have to account for all transfers of molecules in the structure. The driving forces of these transfers are diffusion between compartments and reaction within compartments.

1) Diffusion: The most important quantity to model the diffusion between compartments is the diffusive flux-density

$$\boldsymbol{f} = -D\nabla C(\boldsymbol{r}, t), \tag{22}$$

with D the diffusion coefficient and $C(\boldsymbol{r}, t)$ the concentration at location $\boldsymbol{r}$ and time t. Let us now consider two interconnected compartments (see Fig. 3). We assume that the concentration gradient within one compartment is negligible, and, thus the concentration within one compartment is independent on the location within the compartment. We denote the concentration in the left compartment C_1 and in the right compartment C_2. We approximate $\boldsymbol{f}$ in the channel as

$$\boldsymbol{f} = D\frac{\partial C(\boldsymbol{r}, t)}{\partial x}\boldsymbol{e}_x \approx D\frac{C_1 - C_2}{L}\boldsymbol{e}_x, \tag{23}$$

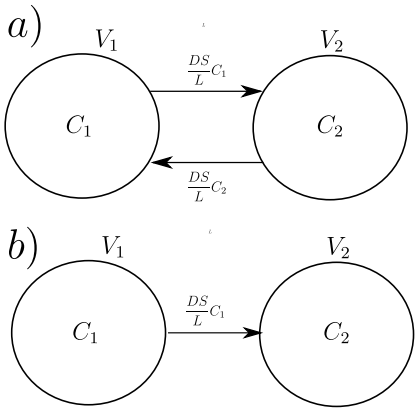

Fig. 4. Types of diffusive coupling: a) bidirectional (regular) diffusion, and b) unidirectional diffusion.

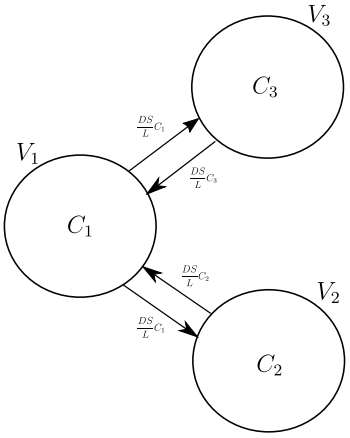

Fig. 5. Three interconnected compartments.

where $\boldsymbol{e}_x$ denotes the unit vector in x-direction. If we assume homogeneous distribution of the concentration in the channel in y and z-direction, we can further write

$$F_{\mathrm{dif}} = D\int_S \boldsymbol{f}\, d\boldsymbol{S} \approx D\int_S \frac{C_1 - C_2}{L}\boldsymbol{e}_x d\boldsymbol{S} \approx \frac{DS(C_1 - C_2)}{L}. \tag{24}$$

The flux F_{dif} describes the molecules exchanged between the two compartments. Its direction depends on the concentration-difference in the compartments, where it flows always from the compartment with higher concentration to the one with lower concentration. How strongly the flux effects the concentration in one compartment depends on the volume of the compartment, which can be described by

$$\frac{dC}{dt} = \frac{d\frac{N}{V}}{dt} = \frac{F_{\mathrm{dif}}}{V}, \tag{25}$$

where the relations $C = \frac{N}{V}$ and $F_{\mathrm{dif}} = \frac{dN}{dt}$ were used. For the case of two coupled compartments depicted in Fig. 3, the changes in concentration can be expressed as

$$\frac{dC_1}{dt} = \frac{DS}{LV_1}(C_2 - C_1) \tag{26a}$$
$$\frac{dC_2}{dt} = \frac{DS}{LV_2}(C_1 - C_2). \tag{26b}$$

If we assume that flux can only occur from compartment 1 to compartment 2 (see Fig. 4b)), we could ignore the effect of C_2 in (26), resulting in

$$\frac{dC_1}{dt} = -\frac{DS}{LV_1}C_1 \tag{27a}$$
$$\frac{dC_2}{dt} = \frac{DS}{LV_2}C_1. \tag{27b}$$

This way of describing systems of connected compartments extends to multiple interconnected compartments in a straightforward manner. For example, for three interconnected compartments (see Fig. 5) the fluxes into each compartment are summed up and we obtain

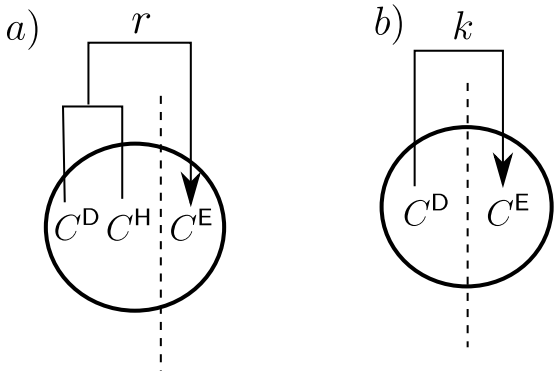

Fig. 6. Illustration of a) second order, and b) first order reaction.

$$\frac{dC_1}{dt} = \frac{DS}{LV_1}(-2C_1 + C_2 + C_3) \tag{28a}$$
$$\frac{dC_2}{dt} = \frac{DS}{LV_2}(C_1 - C_2) \tag{28b}$$
$$\frac{dC_3}{dt} = \frac{DS}{LV_3}(C_1 - C_3). \tag{28c}$$

2) Reactions: Similarly to diffusion, we can also model reactions by fluxes associated with them. Practically, these fluxes however do not leave the compartment, but refer to the conversion of molecules from one type to another (see Fig. 6). In a compartment in which the chemical reaction $\mathsf{D} + \mathsf{H} \to \mathsf{E}$ takes place, this can be modeled as

$$F_{\mathrm{re}} = F_{\mathsf{D}\to\mathsf{E}} = F_{\mathsf{H}\to\mathsf{E}} = VrC^{\mathsf{H}}C^{\mathsf{D}}, \tag{29}$$

with r the reaction coefficient of the second order reaction (unit $\mathrm{m}^3\,\mathrm{s}^{-1}$) and the volume of the compartment under consideration V. For a compartment, in which only reactions (no diffusive fluxes) take place, we can write

$$\frac{dC^{\mathsf{D}}}{dt} = -\frac{F_{\mathrm{re}}}{V} = -rC^{\mathsf{D}}C^{\mathsf{H}} \tag{30a}$$
$$\frac{dC^{\mathsf{H}}}{dt} = -\frac{F_{\mathrm{re}}}{V} = -rC^{\mathsf{D}}C^{\mathsf{H}} \tag{30b}$$
$$\frac{dC^{\mathsf{E}}}{dt} = \frac{F_{\mathrm{re}}}{V} = rC^{\mathsf{D}}C^{\mathsf{H}} \tag{30c}$$

If we assume $C^{\mathsf{H}} \gg C^{\mathsf{D}}$ we can consider $C^{\mathsf{H}} = \hat{C}^{\mathsf{H}} = \mathrm{const.}$

This can be intuitively understood from the following example: Consider the case, where we have 10000 H, but only 10 D molecules. The reaction will stop, when all 10 D have been used up. Since each D reacts with one H after the reaction 9990 H molecules remain. Thus, the number of H molecules has only changed by 0.01% during the entire reaction, which in many cases is negligible. Using this assumption, we convert the nonlinear system of differential equation in (30) into the following linear system of differential equations

$$\frac{dC^{\mathsf{D}}}{dt} = -r\hat{C}^{\mathsf{H}}C^{\mathsf{D}} = -kC^{\mathsf{D}} \tag{31a}$$

$$\frac{dC^{\mathsf{E}}}{dt} = r\hat{C}^{\mathsf{H}}C^{\mathsf{D}} = kC^{\mathsf{D}}, \tag{31b}$$

where $k = r\hat{C}$ is the respective reaction coefficient of the first order reaction. Reconsidering the structure in Fig. 2, we notice that both systems of equations given in (30) and (31) are required. For the reaction in the intermediate defined in (2) and (3), we are in full control of how much C molecules we put into the compartment and, thus, we can always fulfill the condition $C^{\mathsf{H}} \gg C^{\mathsf{D}}$. Hence, for (2) and (3) the model given in (31) is appropriate. Furthermore, we ensure that $k = r^{+}\hat{C}^{\mathsf{C}^{+}} = r^{-}\hat{C}^{\mathsf{C}^{-}}$ holds. This means that if the reactions (2) and (3) happen at different rates r^{+} and r^{-}, we correct the overall reaction rate k by adapting $\hat{C}^{\mathsf{C}^{+}}$ and $\hat{C}^{\mathsf{C}^{-}}$, respectively. On the other hand, since both B^{+} and B^{-} are signaling molecules, we cannot assume that one concentration is larger than the other and, thus, (30) is required to model the reaction in (4).

B. Model of the Computing Structure

Now, we will apply the models derived in the previous subsection to the proposed structure depicted in Fig. 2.

1) States and Initial Conditions for the System of Differential Equations: It is important to note that the size of the system of differential equations grows rapidly with the size of the matrix to be realized. In particular, we need I states for the inlet concentrations of A-type molecules. Furthermore, the $I \times J$ intermediates can hold two types of signaling molecules, namely A and B^{+} or B^{-}. Finally, the J outlet compartments will hold a number of B^{+} and B^{-} molecules. However, we will show that only J state variables are required to fully describe the outlet. Consequently, the number N_{eq} of linear differential equations needed to describe a structure with I inlets and J outlets is given by

$$N_{\mathrm{eq}} = I + 2 \times I \times J + J, \tag{32}$$

which is also the required number of initial conditions. As discussed in Secs. II and III, we assume that initially only the I inlet concentrations are non-zero. Those initial concentrations correspond to the inputs of the computation.

2) Model: Here we derive the differential equations for the structure. We start with the inlet, where Fig. 5 shows an inlet compartment connected to two intermediate compartments and its behavior is described by (28a). In general, every inlet is connected to J outlets. The generalization of (28a) to J compartments is straightforward and reads as

$$\frac{dC^{\mathsf{A}}_{\mathrm{in},i}}{dt} = \frac{DS}{LV_i}\left(-JC^{\mathsf{A}}_{\mathrm{in},i} + \sum_{j=1}^{J} C^{\mathsf{A}}_{i,j}\right). \tag{33}$$

Next, we derive the differential equation for the intermediate compartments. Each intermediate is connected to exactly one inlet and one outlet, as depicted in Fig. 7. The diffusive flux of A-type molecules into the intermediate is $\frac{DS}{L}\left(C^{\mathsf{A}}_{\mathrm{in},i} - C^{\mathsf{A}}_{i,j}\right)$ and the reactive flux is $-kV_{i,j}C^{\mathsf{A}}_{i,j}$. Consequently, we get the differential equation

$$\frac{dC^{\mathsf{A}}_{i,j}}{dt} = \frac{DS}{LV_{i,j}}\left(-C^{\mathsf{A}}_{i,j} + C^{\mathsf{A}}_{\mathrm{in},i}\right) - kC^{\mathsf{A}}_{i,j}. \tag{34}$$

To complete the model of the intermediate compartment, we derive the differential equation of the B-type molecules in the intermediate. Since we assume that the reactions (2) and (3) have the same reaction constant k, we need not make a distinction between positive and negative weights with respect to the dynamics of the process from Fig. 7. We notice that the influx into the B-molecule storage is $kV_{i,j}C^{\mathsf{A}}_{i,j}$ and the efflux is $\frac{DS}{L}C^{\mathsf{B}}_{i,j}$. Consequently, the second equation describing the intermediate compartment is given by

$$\frac{dC^{\mathsf{B}}_{i,j}}{dt} = kC^{\mathsf{A}}_{i,j} - \frac{DS}{LV_{i,j}}C^{\mathsf{B}}_{i,j}. \tag{35}$$

Finally, we model the outlet compartment, which can hold two types of molecules, namely B^{+} and B^{-}. Thus, we need two variables $C^{\mathsf{B}^{+}}_{\mathrm{out},j}$ and $C^{\mathsf{B}^{-}}_{\mathrm{out},j}$. In Fig. 8 all influences on an outlet compartment are depicted. The influx into the outlet comes

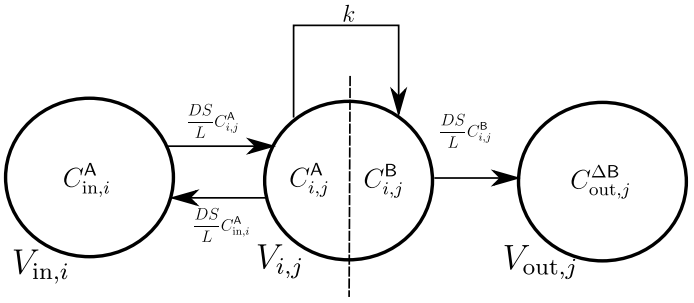

Fig. 7. Illustration of the fluxes at an intermediate compartment.

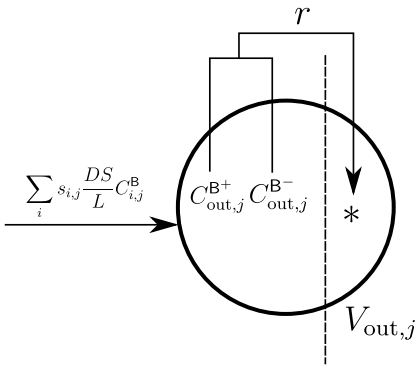

Fig. 8. Illustration of transport and reactions for an outlet compartment.

from all intermediates connected to it. The reactive efflux is given by $rC^{\mathsf{B}^+}_{\mathrm{out},j}C^{\mathsf{B}^-}_{\mathrm{out},j}$, which results in the differential equations for the outlet compartment

$$\frac{dC^{\mathsf{B}^+}_{\mathrm{out},j}}{dt} = -rC^{\mathsf{B}^+}_{\mathrm{out},j}C^{\mathsf{B}^-}_{\mathrm{out},j} + \sum_{i^+}\frac{DS}{LV}C^{\mathsf{B}^+}_{i,j} \tag{36a}$$

$$\frac{dC^{\mathsf{B}^-}_{\mathrm{out},j}}{dt} = -rC^{\mathsf{B}^+}_{\mathrm{out},j}C^{\mathsf{B}^-}_{\mathrm{out},j} + \sum_{i^-}\frac{DS}{LV}C^{\mathsf{B}^-}_{i,j}\,, \tag{36b}$$

where the index i^+ and i^- indicates the summation over all intermediates with positive and negative weights, respectively. It is important to note that (36) is a nonlinear system of differential equations due to the first terms on the right hand side. However, since we are only interested in the difference in the concentrations of B^+ and B^- molecules, we define $C^{\Delta\mathsf{B}}_{\mathrm{out},j} = C^{\mathsf{B}^+}_{\mathrm{out},j} - C^{\mathsf{B}^+}_{\mathrm{out},j}$ and obtain a linear system

$$\frac{dC^{\Delta\mathsf{B}}_{\mathrm{out},j}}{dt} = \sum_{i^+}\frac{DS}{LV}C^{\mathsf{B}^+}_{i,j} - \sum_{i^-}\frac{DS}{LV}C^{\mathsf{B}^-}_{i,j}\,, \tag{37}$$

which can be rewritten using $s_{i,j} \in \{-1, 1\}$ as

$$\frac{dC^{\Delta\mathsf{B}}_{\mathrm{out},j}}{dt} = \sum_{i=1}^{I} s_{i,j}\frac{DS}{LV}C^{\mathsf{B}}_{i,j}, \tag{38}$$

where $C^{\mathsf{B}}_{i,j}$ stands for the respective type of B molecules depending on the sign of $s_{i,j}$, i.e., B^+ for $s_{i,j} = +1$ and B^- for $s_{i,j} = -1$. Please note that by considering only the concentration difference the number of equations required to describe the outlet is reduced from $2J$ to J.

For the sake of clarity, please find below a summary of all equations derived above, which completely characterize the behavior of the proposed structure

$$\frac{dC^{\mathsf{A}}_{\mathrm{in},i}}{dt} = \frac{SD}{LV_i}\left(-JC^{\mathsf{A}}_{\mathrm{in},i}(t) + \sum_{j=1}^{J}C^{\mathsf{A}}_{i,j}\right) \tag{39a}$$

$$\frac{dC^{\mathsf{A}}_{i,j}}{dt} = \frac{SD}{LV_{i,j}}\left(-C^{\mathsf{A}}_{i,j} + C^{\mathsf{A}}_{\mathrm{in},i}\right) - kC^{\mathsf{A}}_{i,j} \tag{39b}$$

$$\frac{dC^{\mathsf{B}}_{i,j}}{dt} = kC^{\mathsf{A}}_{i,j} - \frac{DS}{LV_{i,j}}C^{\mathsf{B}}_{i,j} \tag{39c}$$

$$\frac{dC^{\Delta\mathsf{B}}_{\mathrm{out},j}}{dt} = \sum_{i=1}^{I} s_{i,j}\frac{DS}{LV}C^{\mathsf{B}}_{i,j}. \tag{39d}$$

C. Approximate Time Domain Solution

To get a better understanding of the temporal evolution of all states in the dynamical system given in (39), we present an approximate time domain solution. The derived solution provides insights on the time it takes for a computation to be finished. Furthermore, the influence of the individual parameters (e.g., D, k, etc.) can be deduced.

1) Derivation: The derivation of the approximate solution is based on the same two assumptions we already used for the stochastic model, which are:

- The reaction rate is small (compared to the rate of diffusion), but not zero. Moreover, please note that when we state diffusion is fast or reaction is slow, it is always with respect to the other process.
- We neglect the first time interval, in which diffusion equilibrates the concentration of an inlet and its connected intermediates. It will be short compared to the time the reaction takes since we assumed that diffusion is much faster than reaction

Please note that we also used these assumptions in Sec. III. Similarly we assume that an inlet and its connected intermediate have the same concentration. For the following derivations, we employ a virtual compartment that summarizes one inlet and its connected intermediates, which we refer to as "joint compartment" (see Fig. 9). The volume of the joint compartment is the sum of the volumes of the individual compartments i.e., $V_{\mathrm{tot},i} = V_{\mathrm{in},i} + \sum_j V_{i,j}$ and the concentration of A-type molecules within the joint compartment is equal[3], i.e., $\hat{C}_i = C^{\mathsf{A}}_{\mathrm{in},i} = C^{\mathsf{A}}_{i,j}$. Since at the beginning of the computation only the inlets contain molecules, which evenly distribute among inlet and intermediates (and consequently the joint compartment), we can compute the initial joint compartment concentration as

$$\hat{C}_i^{\mathrm{init}} = \frac{V_{\mathrm{in},i}}{V_{\mathrm{tot},i}}C^{\mathsf{A},\mathrm{init}}_{\mathrm{in},i} = \frac{V_{\mathrm{in},i}}{V_{\mathrm{in},i} + \sum_j V_{i,j}}C^{\mathsf{A},\mathrm{init}}_{\mathrm{in},i} = \alpha_i C^{\mathsf{A},\mathrm{init}}_{\mathrm{in},i}. \tag{40}$$

Next, we accumulate all reactive effluxes out of the joint compartment, which results in a linear first order differential equation

$$\frac{d\hat{C}_i}{dt} = -\frac{k\sum_j V_{i,j}C^{\mathsf{A}}_{i,j}}{V_{\mathrm{tot},i}} = -\frac{k\sum_j V_{i,j}\hat{C}_i}{V_{\mathrm{in},i} + \sum_j V_{i,j}} = -\beta_i\hat{C}_i, \tag{41}$$

with the initial condition given by (40). The solution of (41) can be expressed as

$$\hat{C}_i = \alpha_i e^{-\beta_i t}C^{\mathsf{A},\mathrm{init}}_{\mathrm{in},i}. \tag{42}$$

Thus, (42) provides an approximate solution for the temporal dynamics of the joint compartment and, thus, also for all $C^{\mathsf{A}}_{\mathrm{in},i}$ and $C^{\mathsf{A}}_{i,j}$. Next, we consider the concentration of B-type molecules in the intermediates, i.e., $C^{\mathsf{B}}_{i,j}$. Due to the assumption that diffusion is very fast, each B-type molecule in an intermediate (either B^+ or B^-) is instantly removed and transferred to the respective outlet, from where it cannot return due to the unidirectional transport. Thus, we can approximate $C^{\mathsf{B}}_{i,j} = 0$ for all times t and intermediates (i, j). Since by assumption (justified by the very fast diffusion) the reactive flux $V_{i,j}k\hat{C}_i$ in the intermediate ends up immediately in the respective outlet and one outlet receives multiple fluxes from different intermediates (potentially with different sign $s_{i,j}$),

[3]Note that this equality only holds due to the assumptions above. In general, at the beginning of a computation, the inlet-concentration will be higher than the intermediate concentration (neglected due to the second assumption) and it will always remain slightly higher throughout the computation (neglected due to the first assumption).

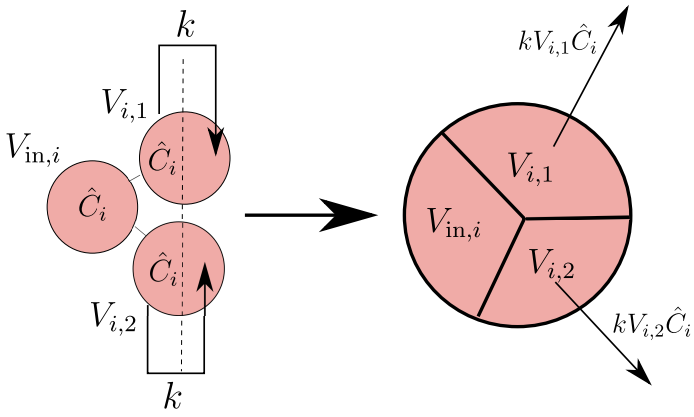

Fig. 9. Conversion from the conventional compartment structure to the joint compartment. Inlet and intermediates are summarized in one homogeneous compartment with the initial concentration proportional to the amount initially placed in an inlet and efflux only occurs out of the intermediates.

we can formulate the differential equation of the concentration difference in a given outlet as follows (see similar derivation (37)):

$$\frac{dC^{\Delta\mathsf{B}}_{\text{out},j}}{dt} = \sum_{i=1}^{I} s_{i,j} k \frac{V_{i,j}}{V} \hat{C}_i. \tag{43}$$

The actual concentration in the outlet can be obtained by substituting (42) into (43) and integrating both sides with respect to t

$$C^{\Delta\mathsf{B}}_{\text{out},j} = \sum_{i=1}^{I} s_{i,j}\gamma_{i,j} C^{\mathsf{A},\text{init}}_{\text{in},i} \left(1 - e^{-\beta_i t}\right), \tag{44}$$

with $\gamma_{i,j} = \frac{V_{i,j}\alpha_i k}{\beta_i V} = \frac{\chi_{i,j} V_{\text{in},i}}{V}$. It is important to note that calculating the steady state of (44) results in (15)

$$\begin{aligned}\lim_{t\to\infty} C^{\Delta\mathsf{B}}_{\text{out},j}(t) &= \sum_{i=1}^{I} s_{i,j}\gamma_{i,j} C^{\mathsf{A},\text{init}}_{\text{in},i} \\ &= \frac{1}{V}\sum_{i=1}^{I} s_{i,j}\chi_{i,j} V_{\text{in},i} C^{\mathsf{A},\text{init}}_{\text{in},i}.\end{aligned} \tag{45}$$

The models presented in this section describes the temporal dynamics of the systems, assuming that diffusion is much faster than reactions. It is an approximate solution to (39) and allows to derive an estimate for the time a computation takes, which will be examined next.

2) Computation Time: From (44), we observe that the solution is a superposition of multiple exponential functions which decay over time. The exponent β_i is a measure for the speed of this decay. It can be shown that after the time $t = \frac{5}{\beta_i}$ the value of this function will not change more than 1%. Hence, the expression

$$\tau_{1,\max} = \max_{i,j} \frac{5}{\beta_i} = \frac{5}{k} \max_{i,j} \left(\frac{V_{\text{in},i}}{\sum_j V_{i,j}} + 1 \right) \tag{46}$$

is a measure for the time duration unless (almost) all molecules have moved to the outlets (i.e., the inlets and intermediates hold (almost) no signaling molecules after this time). Please note that this time constant is based on a linear system of differential equations, which we obtained by a choice of variables (i.e., $C^{\Delta\mathsf{B}}_{\text{out},j} = C^{\mathsf{B}^+}_{\text{out},j} - C^{\mathsf{B}^+}_{\text{out},j}$), that eliminated the non-linear part of the system model stemming from the second order equation[4]. Yet, when we want to obtain an estimate of the overall computation time, we need to reconsider this nonlinear part. Therefore, we make the conservative assumption, that the reaction in the outlet starts only after the linear system has reached steady state (i.e., after waiting for τ_1). Since after his time the concentration in the intermediates is (almost) zero, we can rewrite (36) as

$$\frac{dC^{\mathsf{B}^+}_{\text{out},j}}{dt} = -rC^{\mathsf{B}^+}_{\text{out},j} C^{\mathsf{B}^-}_{\text{out},j} \tag{47a}$$

$$\frac{dC^{\mathsf{B}^-}_{\text{out},j}}{dt} = -rC^{\mathsf{B}^+}_{\text{out},j} C^{\mathsf{B}^-}_{\text{out},j}, \tag{47b}$$

and assume that $C^{\mathsf{B}^+,\text{init}}_{\text{out},j} = C^+_0$ and $C^{\mathsf{B}^-,\text{init}}_{\text{out},j} = C^-_0$ (we use C^+_0 and C^-_0 instead of $C^{\mathsf{B}^+,\text{init}}_{\text{out},j}$ and $C^{\mathsf{B}^-,\text{init}}_{\text{out},j}$ to indicate the respective variable after the linear dynamic has settled). By integrating (47) on both sides with respect to t and equating the right hand sides we obtain

$$C^{\mathsf{B}^+}_{\text{out},j} - C^+_0 = C^{\mathsf{B}^-}_{\text{out},j} - C^-_0. \tag{48}$$

Substituting $\Delta C = C^+_0 - C^-_0$ and (48) into (47) we get[5]

$$\frac{dC^{\mathsf{B}^+}_{\text{out},j}}{dt} = -r(C^{\mathsf{B}^+}_{\text{out},j})^2 + r\Delta C C^{\mathsf{B}^+}_{\text{out},j}, \tag{49}$$

which can be solved using the method of separation of variables and the initial condition $C^{\mathsf{B}^+}_{\text{out},j} = C^+_0$. The solution reads as

$$C^{\mathsf{B}^+}_{\text{out},j} = \frac{\Delta C}{\left(\frac{\Delta C}{C^+_0} - 1\right) e^{-r\Delta C t} + 1}, \tag{50}$$

and can be verified by substituting into (49). The concentration $C^{\mathsf{B}^-}_{\text{out},j}$ can be obtained by subtracting ΔC from (50). From (50) we notice that for $\Delta C > 0$ the state of $C^{\mathsf{B}^+}_{\text{out},j}$ tends towards ΔC as time approaches infinity, since in this case only B^+ molecules remain (see (4)). If $\Delta C < 0$, the state of $C^{\mathsf{B}^+}_{\text{out},j}$ approaches zero as time approaches infinity, since all B^+ type molecules are used up. Moreover, it can be observed that the only time dependent expression is $e^{-r\Delta C t}$. Thus, we can define a time constant which is a measure for the time a computation needs to finish and is given by

$$\tau_2 \propto \frac{1}{r\Delta C}. \tag{51}$$

As expected (since the system is non-linear), the time constant depends on the input concentration. To get rid of ΔC, we use the fact that the concentration can never become smaller than one molecule per unit volume (i.e., there are no half

[4]Physically this means that we assume that we are able to measure B^+, B^- and $*$ all at the same time. Under this assumption, once all molecules have arrived in the outlet compartment their difference (i.e., the outcome) is fixed and can be measure. If we are however only able to measure B^+ and B^-, then we need to wait until the second order reaction has settled and only one species has remained.

[5]The following derivations are valid for $\Delta C \neq 0$. For this special case, the same condition can be obtained. The derivation will be omitted for the sake of compactness.

molecules). Thus, we set $\min\Delta C = \frac{1}{V_{\max}}$ and obtain the estimate

$$\tau_{2,\max} \propto \frac{V_{\max}}{r}. \tag{52}$$

Finally, the overall computation time can be calculated as follows:

$$\tau = \frac{5}{k}\max_{i,j}\left(\frac{V_{\mathrm{in},i}}{\sum_j V_{i,j}} + 1\right) + \frac{V_{\max}}{r} \tag{53}$$

V. Advanced Analysis and Design Algorithms

So far, we have presented two types of models. The stochastic model derived in Sec. III relates the initial inlet concentration to the final outlet concentration (i.e., (16)), but does not consider the temporal evolution of the states in the compartments. Moreover, this model is only valid, if we can assume that the reactions in all compartments are slow compared to the diffusive processes. On the other hand, the dynamical model derived in Sec. IV (cf. (39)) describes the temporal dynamics of all states in the structure for all times without any constraints. However, we have not yet established a relation between initial inlet and final outlet concentration. Thus, in this section, we will first derive this relation and relate it to the expected value of the stochastic model derived in Sec. III. We will show that the final states of the two models converge towards each other under the assumption that reaction is much slower than diffusion. If this assumption is violated, the stochastic model becomes invalid and, thus, the way of finding the volumes obtained by this model (i.e., (20)) becomes invalid as well. Thus, based on the dynamical model (39), we will show how to derive the compartment volumes in this case.

A. Steady State of the Dynamical Model

The goal of this subsection is to relate the initial inlet concentration of the dynamical model (39) to its final outlet concentration, which defines the matrix multiplication. Therefor, we use the final value theorem of the Laplace transform, which reads as

$$C_{\mathrm{out},j}^{\Delta\mathsf{B},\mathrm{fin}} = \lim_{s\to 0} s\mathcal{L}\{C_{\mathrm{out},j}^{\Delta\mathsf{B}}\} = \lim_{s\to 0} s\widetilde{C}_{\mathrm{out},j}^{\Delta\mathsf{B}}(s), \tag{54}$$

with s the Laplace variable and the tilde indicating that a variable is in the Laplace domain. To obtain $\widetilde{C}_{\mathrm{out},j}^{\Delta\mathsf{B}}(s)$, we transform (39) into the Laplace domain, resulting in the following linear system of algebraic equations

$$s\widetilde{C}_{\mathrm{in},i}^{\mathsf{A}}(s) - C_{\mathrm{in},i}^{\mathsf{A},\mathrm{init}} = \frac{SD}{LV_i}\left(-J\widetilde{C}_{\mathrm{in},i}^{\mathsf{A}}(s) + \sum_{j=1}^{J}\widetilde{C}_{i,j}^{\mathsf{A}}(s)\right) \tag{55a}$$

$$s\widetilde{C}_{i,j}^{\mathsf{A}}(s) - 0 = \frac{SD}{LV_{i,j}}\left(-\widetilde{C}_{i,j}^{\mathsf{A}}(s) + \widetilde{C}_{\mathrm{in},i}^{\mathsf{A}}(s)\right) - k\widetilde{C}_{i,j}^{\mathsf{A}}(s) \tag{55b}$$

$$s\widetilde{C}_{i,j}^{\mathsf{B}}(s) - 0 = k\widetilde{C}_{i,j}^{\mathsf{A}}(s) - \frac{DS}{LV_{i,j}}\widetilde{C}_{i,j}^{\mathsf{B}}(s) \tag{55c}$$

$$s\widetilde{C}_{\mathrm{out},j}^{\Delta\mathsf{B}}(s) = \sum_{i=1}^{I} s_{i,j}\frac{DS}{LV}\widetilde{C}_{i,j}^{\mathsf{B}}(s). \tag{55d}$$

By solving this linear equation system with respect to $\widetilde{C}_{\mathrm{out},j}^{\Delta\mathsf{B}}(s)$, we obtain

$$\widetilde{C}_{\mathrm{out},j}^{\Delta\mathsf{B}}(s) = \frac{1}{s}\frac{SD}{LV}\sum_{i=1}^{I}\frac{s_{i,j}kSDC_{\mathrm{in},i}^{\mathsf{A},\mathrm{init}}}{Q_{i,j}}, \tag{56}$$

with

$$Q_{i,j} = \left(s + \frac{SD}{LV_{\mathrm{in},i}}\left(J - \sum_{k=1}^{J}\frac{SD}{sLV_{i,j} + SD + kLV_{i,j}}\right)\right)\times \left(s + \frac{SD}{LV_{i,j}}\right)\left(sLV_{i,j} + SD + kLV_{i,j}\right). \tag{57}$$

Substituting this result into (54) results in

$$C_{\mathrm{out},j}^{\Delta\mathsf{B},\mathrm{fin}} = \frac{1}{V}\sum_{i=1}^{I}\frac{s_{i,j}V_{\mathrm{in},i}V_{i,j}G_{i,j}}{\sum_{k=1}^{J}V_{i,k},G_{i,k}}C_{\mathrm{in},i}^{\mathsf{A},\mathrm{init}}, \tag{58}$$

with

$$G_{i,j} = \frac{SD}{SD + kLV_{i,j}}. \tag{59}$$

It is important to note that for $G_{i,j} = 1$, (58) corresponds to the input-output relation derived in Sec. III (cf. (15)). From (59) it can be seen that $G_{i,j} = 1$ holds if

$$\max(V_{i,j})kL \ll SD. \tag{60}$$

This condition[6] allows us to determine the range, where the naive design algorithm for determining the compartment volumes given in (20) is valid. In addition, (60) allows the derivation of the scale, for which the proposed concept is applicable. This can be seen by reformulating (60) that the left hand side depends only on quantities defined by the scale, while the right hand side only depends on the properties of the involved substances

$$\frac{\max(V_{i,j})L}{S} \ll \frac{D}{k}. \tag{61}$$

This relation states that increasing k lowers the upper bound on the size of the structure. On the other hand, (46) states that for larger k the computation gets faster. Combining these two statements, we can conclude that the smaller the structure gets[7], the larger k can be chosen (while still fulfilling (60)) and the faster the computation will be. Another important consequence is that for a given desired computation time, the possible pool of chemicals (corresponding to the range of reaction rates) increases with decreasing structure size. Thus, the proposed structure is especially suitable for the micro-scale and below. Please note however that the structure cannot be shrinked arbitrarily far due to the increased computation noise for smaller scales (see (21)).

[6]Please note that (60) is just the condition that the reaction time scale $\tau_{\mathrm{re}} = \frac{1}{k}$ is much larger than the maximum diffusion time $\tau_{\mathrm{dif}} = \frac{\max(V_{i,j})L}{SD}$, which can be obtained simply by rearranging.

[7]A smaller structure means that a given structure is shrinked equally along all axis (x, y, and z). Hence, the volume, channel area, and channel length decrease with the third, second, and first power of the reduction factor, respectively.

B. Advanced Design Algorithm

In the previous subsection we derived a condition (i.e., (60)), under which the models derived in Sec. III are valid. In this case, the naive design algorithm for determining the compartment volumes given in (20) for arbitrary matrix entries can be applied. It is recommended to design the architecture in a way that (60) is fulfilled(note, how in (17) neither S nor L plays a role. This allows for great geometrical flexibility when building the structure). However, if (60) could be not fulfilled, we give the reader an understanding of how to deal with a violation of this condition in the following. Therefore, we consider a simple example of cubic volumes connected by cubic channels. To give the reader an outlook on future challenges, we furthermore show, how to incorporate a side condition, that is, the channel diameters should be smaller than the volume diameter. Hence, the two conditions we would like to simultaniously fulfill are:

- Main condition: Find the volumes of the structure such that it realizes $\boldsymbol{M}$ taking into consideration k and D.
- Geometrical constraint: Make sure that the diameter of all volumes is much larger than the channel diameter.

The algorithm to derive the compartment models can be derived based on (58) and some geometrical considerations. Without loss of generality, we will assume that all volumes and channels are cube-shaped. We formulate the geometrical constraint from above as

$$V_{\text{channel}} = \delta^3 = \frac{V_{\min}}{\kappa}, \tag{62}$$

where κ is a number much larger than one (typically we choose $\kappa = 1000$), $V_{\min}$ is the smallest volume in the structure, and δ is the channel length, width and height. It follows immediately that $S = \delta^2$ and $L = \delta$. To enforce the main condition, we use (58). We notice that $C_{\text{out},j}^{\Delta\text{B},\text{fin}}$ is a weighted sum over $C_{\text{in},i}^{\text{A},\text{init}}$ and identify the matrix weight

$$M_{j,i} = \frac{s_{i,j} V_{\text{in},i} V_{i,j} G_{i,j}}{\sum_{k=1}^{J} V V_{i,k}, G_{i,k}}. \tag{63}$$

Since the denominator for different j and similar i is the same, we can get rid of the denominator by defining a ratio of the weights

$$\frac{M_{j,i}}{M_{k,i}} = \frac{s_{i,j} V_{i,j} G_{i,j}}{s_{i,k} V_{i,k} G_{i,k}}. \tag{64}$$

Substituting the definition of $G_{i,j}$ (see (59)) and $s_{i,j}$ (from (20c)) and then solving for $V_{i,k}$ results in

$$V_{i,k} = \frac{V_{i,j} \frac{|M_{k,i}|}{|M_{j,i}|}}{1 + \frac{rL}{DS} V_{i,j} \left(1 - \frac{|M_{k,i}|}{|M_{j,i}|}\right)}. \tag{65}$$

Thus, if we know one intermediate volume $V_{i,j}$, we can calculate all others from it. However, due to the negative sign in the denominator, the volume can in general become negative, which does not make sense from a physical point of view. To avoid this problem, we set $V_{i,j} = V_{\max}$, where $V_{\max}$ is the largest intermediate volume in the structure. This volume is a required input for the design algorithm. Since (65) can be applied to each column of $\boldsymbol{M}$, the first step in our algorithm is to set the volume corresponding to the largest weight in each column of $\boldsymbol{M}$ to $V_{\max}$. Then, we can calculate the other intermediate volume of the structure by

$$V_{i,k} = \frac{V_{\max} \frac{|M_{k,i}|}{\max |M_{j,i}|}}{1 + \frac{rL}{DS} V_{\max} \left(1 - \frac{|M_{k,i}|}{\max |M_{j,i}|}\right)}. \tag{66}$$

It is important to note that now we will never get a negative results, since we started by the largest weight and, thus, $\frac{M_{k,i}}{\max |M_{j,i}|} < 1$. If we would not need to consider the geometrical constraint, we would be already done at this point. To be able to enforce this condition, however, we need to derive the smallest volume $V_{\min}$ (cf. (62)). This can be again obtained through (66), resulting in

$$V_{\min} = \frac{V_{\max} \min\limits_{i,k} \frac{|M_{k,i}|}{\max\limits_{j} |M_{j,i}|}}{1 + \frac{rL}{DS} V_{\max} \left(1 - \min\limits_{i,k} \frac{|M_{k,i}|}{\max\limits_{j} |M_{j,i}|}\right)}. \tag{67}$$

Substituting into (62) gives

$$\delta^3 = \frac{1}{\kappa} \frac{V_{\max} \min\limits_{i,k} \frac{|M_{k,i}|}{\max\limits_{j} |M_{j,i}|}}{1 + \frac{r\delta}{D\delta^2} V_{\max} \left(1 - \min\limits_{i,k} \frac{|M_{k,i}|}{\max\limits_{j} |M_{j,i}|}\right)}. \tag{68}$$

When solving this equation, we end up with an expression of the form

$$\delta^3 + a\delta^2 - b = 0 \tag{69}$$

with $a > 0$ and $b > 0$. Since $b > 0$ the expression on the left hand side is less than zero for $\delta = 0$. Thus, there is always at least one positive solution for δ (in fact, it can be shown by the rule of Descartes [15], that there is exactly one such solution). Finally, we have to choose the dimensions of the inlet and outlet compartments. As we see from (58), we again only care about the ratio of the two, thus they can be always chosen in a way such that they satisfy the above conditions. Note that at this point all $V_{i,j}$ and $G_{i,j}$ are known. Thus, we can get the ratio of $V_{\text{in},i}$ and V from (63) as

$$\theta_i = \frac{V_{\text{in},i}}{V} = M_{j,i} \frac{\sum_{k=1}^{J} V_{i,k}, G_{i,k}}{s_{i,j} V_{i,j} G_{i,j}}, \tag{70}$$

where we only need to choose one pair of indices (j, i) for each column of $\boldsymbol{M}$. After having computed the fraction for all columns, we know the smallest θ_i. If it is larger than 1, we set the V to a value $V_0 \geq V_{\min}$ and calculate all $V_{\text{in},i}$ from V using (70). Otherwise, we set the $V_{\text{in},i}$ to the V_0, calculate V from it using (70) and use the obtained V to calculate all other $V_{\text{in},i}$ again from (70). This way, all inlet and outlet volumes are definitely larger than the smallest intermediate and thus the overall solution will satisfy the geometrical constraint. The pseudo-code shown in Alg. 1 summarizes the algorithm for determining the compartment volumes discussed above, referring to as Advanced Design Algorithm. Please note that we made the choice, that the smallest of inlet or outlet compartments should be $V_{\min}$. Other choices would of course be also possible.

Algorithm 1 Advanced Design Algorithm

Input: k, D, $V_{\max}$, $\boldsymbol{M}$, κ
Output: List of Volumes
Initialization :
for i in columns of $\boldsymbol{M}$ **do**
  $k \leftarrow \underset{j}{\operatorname{argmax}} M_{j,i}$
  Set $V_{i,k} \leftarrow V_{\max}$
end for
Calculate δ solving (68)
$S \leftarrow \delta^2$
$L \leftarrow \delta$
for j in rows of $\boldsymbol{M}$ and i in columns of $\boldsymbol{M}$ **do**
  Compute $V_{i,j}$ from (65)
end for
$\theta \leftarrow \min_i \frac{V_{\mathrm{in},i}}{V} = M_{j,i} \frac{\sum_{k=1}^{J} V_{i,k} G_{i,k}}{s_{i,j} V_{i,j} G_{i,j}}$
if $\theta > 1$ **then**
  Set $V \leftarrow V_{\min}$
else
  Calculate $V \leftarrow \frac{V_{\min}}{\theta}$
end if
for i in columns of $\boldsymbol{M}$ **do**
  $V_{\mathrm{in},i} = \theta_i V$ with θ_i obtained from the r.h.s. from (70)
end for
return All $V_{\mathrm{in},i}$, $V_{i,j}$ and V

VI. Simulation Results

In this section, we validate the functionality and the mathematical models of the proposed matrix multiplication structure using a microscopic-mesoscopic hybrid simulation (MMS). We study a matrix multiplication with a 3×2 matrix[8] and consider two scenarios, one fulfilling and one violating the condition given in (60).

A. Parameters and Simulation Scenarios

We consider the multiplication of a two-dimensional input vector $\boldsymbol{C}_{\mathrm{in}}$ with a 3×2 matrix $\boldsymbol{M}$, resulting in a three-dimensional output vector $\boldsymbol{C}_{\mathrm{out}}$. The weights of the matrix were generated randomly (in the range $[-5, 5]$ rounded to one decimal place) and the matrix we used for the following studies is given by

$$\boldsymbol{M} = \begin{bmatrix} -3.5 & 3.7 \\ -0.8 & -2.0 \\ -4.4 & 2.4 \end{bmatrix}. \tag{71}$$

Similar, the values of the input vectors were generated randomly (in the range $[0, 2]$). For our studies we used two different vectors, which are given by

$$\boldsymbol{C}_{\mathrm{in}}^{(1)} = \begin{bmatrix} 0.6 & 0.4 \end{bmatrix}^{\mathrm{T}} \times 10^{21} \, \frac{\mathrm{molecules}}{\mathrm{m}^3} \tag{72}$$

and

$$\boldsymbol{C}_{\mathrm{in}}^{(2)} = \begin{bmatrix} 1.1 & 0.2 \end{bmatrix}^{\mathrm{T}} \times 10^{21} \, \frac{\mathrm{molecules}}{\mathrm{m}^3}. \tag{73}$$

[8]Other matrix dimensions will lead to similar conclusions, but omitted here due to the lack of space.

TABLE I
Parameter for two simulation scenarios

Parameter	Value (scenario 1)	Value (scenario 2)
k	$1 \, \frac{1}{\mathrm{s}}$	$20 \, \frac{1}{\mathrm{s}}$
D	$10^{-8} \, \frac{\mathrm{m}^2}{\mathrm{s}}$	$10^{-9} \, \frac{\mathrm{m}^2}{\mathrm{s}}$

TABLE II
Dimensions of the structure determined by the naive and advanced design algorithm

Parameter	Value (naive design)	Value (advanced design)
L	$0.1\,\mu\mathrm{m}$	$0.076\,\mu\mathrm{m}$
S	$0.01\,\mu\mathrm{m}^2$	$0.0058\,\mu\mathrm{m}^2$
V	$1\,\mu\mathrm{m}^3$	$0.44\,\mu\mathrm{m}^3$
$V_{1,1}$	$3.5\,\mu\mathrm{m}^3$	$3.13\,\mu\mathrm{m}^3$
$V_{1,2}$	$0.8\,\mu\mathrm{m}^3$	$0.44\,\mu\mathrm{m}^3$
$V_{1,3}$	$4.4\,\mu\mathrm{m}^3$	$5\,\mu\mathrm{m}^3$
$V_{2,1}$	$3.7\,\mu\mathrm{m}^3$	$5\,\mu\mathrm{m}^3$
$V_{2,2}$	$2\,\mu\mathrm{m}^3$	$1.68\,\mu\mathrm{m}^3$
$V_{2,3}$	$2.4\,\mu\mathrm{m}^3$	$2.22\,\mu\mathrm{m}^3$
$V_{\mathrm{in},1}$	$8.7\,\mu\mathrm{m}^3$	$3.81\,\mu\mathrm{m}^3$
$V_{\mathrm{in},2}$	$8.1\,\mu\mathrm{m}^3$	$3.54\,\mu\mathrm{m}^3$

We expect the following concentration in the outlets as the result of the matrix multiplication

$$\begin{aligned} \boldsymbol{C}_{\mathrm{out}}^{(1)} &= \boldsymbol{M}\boldsymbol{C}_{\mathrm{in}}^{(1)} \\ &= \begin{bmatrix} 3.08 & -3.28 & 0.72 \end{bmatrix}^{\mathrm{T}} \times 10^{21} \, \frac{\mathrm{molecules}}{\mathrm{m}^3} \end{aligned} \tag{74}$$

and

$$\begin{aligned} \boldsymbol{C}_{\mathrm{out}}^{(2)} &= \boldsymbol{M}\boldsymbol{C}_{\mathrm{in}}^{(2)} \\ &= \begin{bmatrix} -3.11 & -1.28 & -4.36 \end{bmatrix}^{\mathrm{T}} \times 10^{21} \, \frac{\mathrm{molecules}}{\mathrm{m}^3}. \end{aligned} \tag{75}$$

For our studies we consider two different scenarios. The parameters (r and D) for the first and second scenario were chosen such that the condition given in (60) is fulfilled or violated (cf. Tab. I). In the first scenario, the naive design algorithm for calculating the volumes defined by (20) can be applied and the resulting dimensions are summarized in Tab. II. In the second scenario, the condition (60) was intentionally violated, which will show the effect of such a violation on the naive design algorithm. It is important to note that the naive design algorithm does not utilize k or D, so it will still yield the same dimensions as in the first scenario. However, the advanced design algorithm given in Alg. 1 takes those values into account and the resulting volumes with $V_{\max} = 5\,\mu\mathrm{m}^3$ and $\kappa = 1000$ are summarized in Tab. II.

B. Simulation Environment

For the MMS we used the AcCoRD simulator presented in [16]. For convenience of implementation, all volumes and connecting channels were chosen of cubic shape. The length, height, and width of each compartment was chosen such that the volume had the value specified in Tab. II. Channel length and width are presented in the same table. With the microscopic simulation method the movement of the individual molecules can be simulated, which is referred to as particle-based simulation (PBS). This simulation method updates the

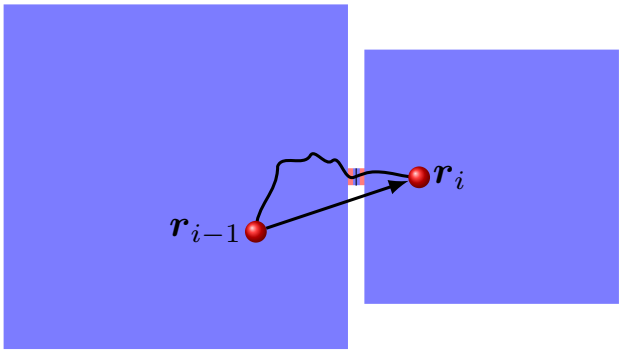

Fig. 10. Comparison of actual molecule trajectory and linear interpolation.

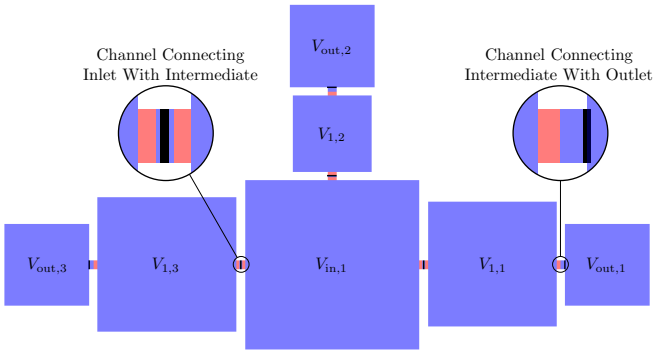

Fig. 11. Two-dimensional view of the AcCoRD simulation setup for one inlet compartment.

molecule position at each time step, by adding a Gaussian random variable [17]. It is important to note that it only gives a straight-line interpolation between the molecule position at the beginning and end of the time step instead of the actual molecule trajectory. Thus, it may happen that a straight-line interpolation leads to a reflection, while in reality, the molecule propagates from one compartment to another, as illustrated in Fig. 10. To overcome this problem the time step Δt needs to be set very small. As a rule of thumb, the root mean square distance covered in a time step (cf. Appendix A) should be much smaller than the smallest dimension of a structure [16]. For the parameter scenario 1 this condition reads

$$\begin{aligned} \sqrt{2D\Delta t} &\ll L \\ \Delta t &\ll 5 \times 10^{-7}\,\text{s}, \end{aligned} \tag{76}$$

since the smallest dimension is given by the channel length. Satisfying (76) is challenging, as the necessity for extremely small time steps makes simulations impractical due to the increased computational effort. Thus, a different approach must be used for the channels, while the compartments can be simulated with the microscopic simulation method, as they are considerably larger than the channel. Our chosen approach involves simulating the channels of the structure using the mesoscopic simulation method, which allows for an accurate simulation of the transition between two compartments. This is because, for microscopic-mesoscopic interfaces, the probability that a molecule may have entered the mesoscopic region (i.e., channel) during a time step is taken into account. Consequently, provided a molecule is outside the channel at the end of the time step, it can be manually placed in the channel based on this probability. However, it is important to note that the mesoscopic simulation method no longer simulates each molecule individually but only the number of molecules per subvolume[9]. Nevertheless, this method provides accurate results as long as the subvolumes are small, which is fulfilled for the channels. However, it is not possible to simulate the entire channel in the mesoscopic region since the AcCoRD simulator does not support the correct functionality of membranes, required for unidirectional transport, at mesoscopic interfaces. Thus, membranes must be placed adjacent to microscopic regions. Fig. 11 illustrates the two-dimensional view of the simulation setup for one inlet, considering the naive design algorithm[10]. The blue and red colored regions are simulated using the microscopic and mesoscopic simulation method, respectively. Moreover, membranes are represented by black lines. For the microscopic simulations, a time step of $\Delta t = 10^{-6}\,\text{s}$ and $\Delta t = 10^{-7}\,\text{s}$ is used for scenario 1 and 2, respectively. Due to the longer simulation duration required for scenario 1, caused by the slower reaction rate k, the time step is chosen larger to obtain a reasonable computational effort.

C. Results of Scenario 1

The simulation parameters for scenario 1 can be found in Tabs. I and II. The simulations were carried out as long as necessary, i.e., until the computation time defined in (46) was reached[11]. For the used simulation parameters the computation time is given by

$$\tau_{1,\max} = \frac{5}{k} \max_{i,j} \left(\frac{V_{\text{in},i}}{\sum_j V_{i,j}} + 1 \right) = 10\,\text{s}. \tag{77}$$

During the simulation the concentration $C_{\text{out}}^{(\text{i})}$ in each outlet was recorded. The results for the dynamical model (cf. (39)) were obtained numerically using Matlab. In Fig. 12 the comparison of the MMS and the dynamic model is shown, while Fig. 13 presents the comparison of the approximate (cf. (44)) and dynamic model. In both figures, the results for the first and second input vector are marked in blue and red, respectively. The comparison in Fig. 12 reveals a good agreement between the MMS and the results of the dynamic model. Moreover, Fig. 13 demonstrates that the dynamical and approximate model match very well, since in this scenario the condition in (60) is fulfilled. Finally, we observe that the simulation and model results converge towards the desired outcome calculated in (74) and (75), which validates the matrix multiplication given in (5).

[9]The details of this simulation method can be found in [16].

[10]Please note that due to the statistical independence of the concentrations in the outlet stemming from different inlets, each inlet can be simulated individually.

[11]Since it is assumed that the reaction (4) occurs instantaneously, τ_2 must not be added to the total computation time.

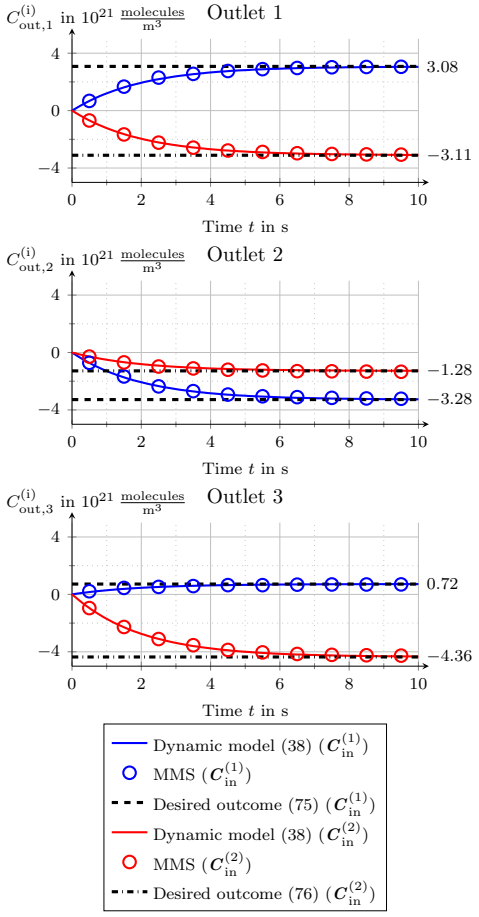

Fig. 12. Simulation results for scenario 1: Comparison of MMS and dynamic model.

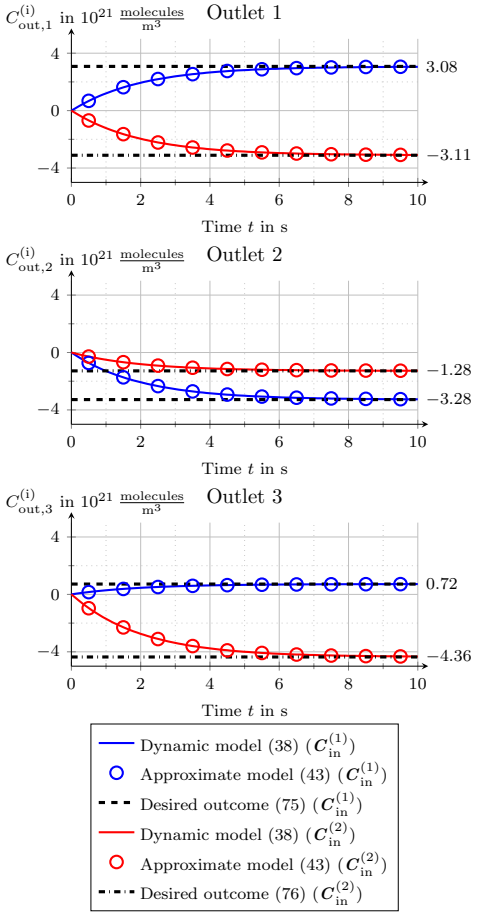

Fig. 13. Simulation results for scenario 1: Comparison of approximate and dynamic model.

D. Results of Scenario 2

The simulation parameters for scenario 2 are summarized in Tabs. I and II and were chosen that the condition in (60) is violated. Thus, we expect that the volumes obtained by the naive design algorithm will lead to an insufficient performance, which justifies the utilization of the advanced design algorithm given in Alg. 1. The MMS and the results for the dynamical model were obtained in a similar way as for scenario 1. Fig. 14 shows the concentration in the three outlets for the first input vector $\mathbf{C}^{(1)}_{\text{in}}$. We observe a very good match between the MMS and the results of the dynamical model. Moreover, we notice that with the advanced design algorithm the results converge towards the desired outcome given in (74), while the naive design algorithms do not converge. Thus, the advanced design algorithm is able to eliminate the influence of the violation of the condition in (60), which shows its importance for this scenario.

VII. Conclusion Outlook

In this paper, we proposed a novel reaction-diffusion-based compartment architecture that is capable of carrying out matrix multiplications in the micro and nano-domain. The architecture is capable of realizing arbitrary matrices with both positive and negative weights, which can be set independently through adjusting the volumes of the compartments. We derived a stochastic model and an approximate dynamical model that shows the steady state and temporal behavior of the system, assuming slow reaction and fast diffusion. The approximate model was further used to estimate the computation speed of the structure. Then we presented a differential equation model which fully characterizes the dynamic behavior of the system, without any constraints (i.e., reaction and diffusion may operate on the same time scale). Based on the aforementioned models we defined two design algorithms for the compartment volumes given arbitrary matrix entries. We validated the functionality of the proposed architecture and the proposed models by a microscopic-mesoscopic hybrid simulation. The presented structure and the design algorithms can be adapted to form neural networks and, thus, enable micro/nano-scale artificially engineered neural networks. This, along with a practical realization of the proposed concept is the scope of future research.

Acknowledgement

This work has been supported by the ”University SAL Labs” initiative of Silicon Austria Labs (SAL) and its Austrian partner universities for applied fundamental research for electronic based systems.

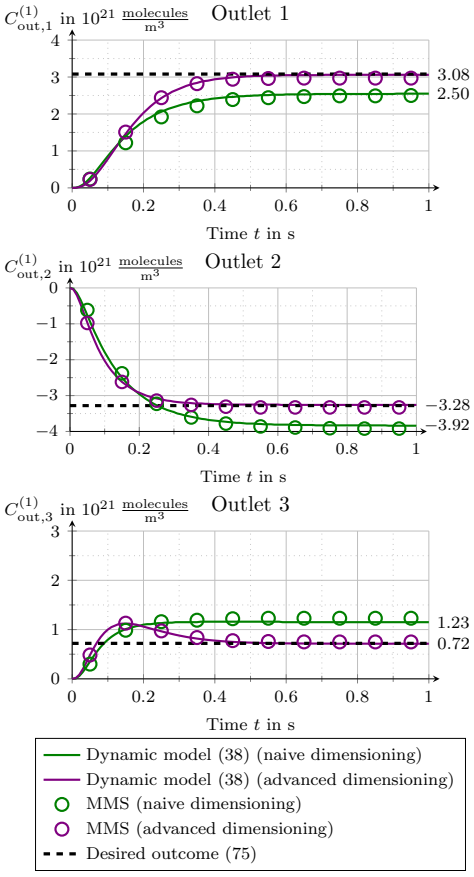

Fig. 14. Simulation results for scenario 2: Comparison of different naive and advanced dimensioning.

REFERENCES

[1] S. Angerbauer *et al.*, "Novel nano-machine architecture for machine learning in the iobnt," accepted for publication GLOBECOM 2023 - 2023 IEEE Global Communications Conference, [Online].https://doi.org/10.36227/techrxiv.23283686.v1.

[2] J. Caird, K. Hinds, I. Kwan, and J. Thomas, *A systematic rapid evidence assessment of late diagnosis*. Social Science Research Unit, 2012.

[3] Y. K. Alotaibi and F. Federico, "The impact of health information technology on patient safety," *Saudi medical journal*, vol. 38, no. 12, p. 1173, 2017.

[4] K. A. Lynch, T. M. Atkinson, A. D. Omisore, O. Famurewa, O. Olasehinde, O. Odujoko, O. I. Alatise, A. Egberongbe, T. P. Kingham, E. A. Morris *et al.*, "Developing a technology acceptability and usage survey (taus) for mhealth intervention planning and evaluation in nigeria: Pilot study," *JMIR Formative Research*, vol. 6, no. 4, p. e34035, 2022.

[5] M. Kuscu and B. D. Unluturk, "Internet of bio-nano things: A review of applications, enabling technologies and key challenges," *ArXiv*, vol. abs/2112.09249, 2021.

[6] I. F. Akyildiz *et al.*, "The internet of bio-nano things," *IEEE Commun. Mag.*, vol. 53, no. 3, pp. 32–40, 2015.

[7] P.-Q. Ma *et al.*, "A highly integrated DNA nanomachine operating in living cells powered by an endogenous stimulus," *Chemical Science*, vol. 9, no. 13, pp. 3299–3304, 2018.

[8] N. Farsad, H. B. Yilmaz, A. Eckford, C.-B. Chae, and W. Guo, "A comprehensive survey of recent advancements in molecular communication," *IEEE Communications Surveys and Tutorials*, vol. 18, no. 3, pp. 1887–1919, 2016.

[9] K. Sarkar *et al.*, "A single layer artificial neural network type architecture with molecular engineered bacteria for reversible and irreversible computing," *Chemical Science*, vol. 12, no. 48, pp. 15 821–15 832, 2021.

[10] S. Balasubramaniam *et al.*, "Realizing Molecular Machine Learning Through Communications for Biological AI," *IEEE Nanotechnol. Mag.*, pp. 1–11, 2023.

[11] D. Bi and Y. Deng, "Digital Signal Processing for Molecular Communication via Chemical-Reaction-Based Microfluidic Circuits," *IEEE Commun. Mag.*, vol. 59, no. 5, pp. 26–32, 2021.

[12] M. Vasić, C. Chalk, A. Luchsinger, S. Khurshid, and D. Soloveichik, "Programming and training rate-independent chemical reaction networks," *Proceedings of the National Academy of Sciences*, vol. 119, no. 24, p. e2111552119, 2022.

[13] D. Soloveichik, G. Seelig, and E. Winfree, "Dna as a universal substrate for chemical kinetics," *Proceedings of the National Academy of Sciences*, vol. 107, no. 12, pp. 5393–5398, 2010.

[14] D. W. Scott, *Statistics: a concise mathematical introduction for students, scientists, and engineers*. John Wiley & Sons, 2020.

[15] R. N. Aufmann and R. D. Nation, *Algebra and Trigonometry*. Cengage Learning, 2014.

[16] A. Noel *et al.*, "Simulating with accord: Actor-based communication via reaction–diffusion," *Nano Communication Networks*, vol. 11, pp. 44–75, 2017. [Online]. Available: https://www.sciencedirect.com/science/article/pii/S1878778916300618

[17] N. Farsad, H. B. Yilmaz, A. Eckford, C.-B. Chae, and W. Guo, "A comprehensive survey of recent advancements in molecular communication," *IEEE Commun. Surv. Tutor.*, vol. 18, 02 2016.

APPENDIX A
CONDITION FOR HOMOGENEOUS CONCENTRATION DISTRIBUTION WITHIN COMPARTMENTS

In this section, we justify the use of a compartment model to describe the physical behavior of proposed the architecture. The underlying assumption for the utilization of compartment models is, that the concentration within one compartment is uniform, and thus, we only need one state variable to define the concentration in the compartment. In order to ensure this condition we consider the one-dimensional diffusion equation [8]

$$\frac{\partial c(x,t)}{\partial t} = D\frac{\partial^2 c(x,t)}{\partial x^2}, \tag{78}$$

which has the following solution in the unbounded space

$$c(x,t) = \frac{K}{\sqrt{4\pi Dt}} e^{-\frac{x^2}{4Dt}}. \tag{79}$$

If we interpret this result as the probability of observing a molecule ($K = 1$) at location x and choose the origin of our coordinate system in the center of a compartment, we notice that the variance of this distribution is $2Dt$. Thus, the time until a molecules has been displaced by a distance d is $\sqrt{2Dt}$. In the case of a compartment, we do have boundary conditions in some areas (i.e., the molecules can leave the compartments only through the channels and not the walls). Nevertheless, the influence of the boundaries will become visible, after the molecules has diffused from the center to the boundaries, for which reason, we define

$$\tau_{\text{comp}} = \frac{a^2}{2D}, \tag{80}$$

as a measure for the time it takes for a molecule to diffuse through the compartment. Thereby a indicates the largest diameter of a compartment. On the other hand, the rate at which molecules are entering from the other compartments for two interconnected compartments can be obtained from (27) as

$$\tau_{\text{chan}} = \frac{VL}{DS}. \tag{81}$$

If $\tau_{\text{comp}} \ll \tau_{\text{chan}}$, we conclude that molecules have sufficient time to spread through a compartment before new molecules

arrive in the compartment. Hence, uniform concentration in a compartment can be ensured by the following condition

$$\frac{a^2}{2} \ll \frac{LV_{\min}}{S}. \tag{82}$$

Note, that this condition is of purely geometrical nature, which means it can be fulfilled by designing the shape of the structure accordingly.